

SUPPORTING INFORMATION SECTION

Kinetics and Mechanisms of Cr(VI) Formation via the Oxidation of Cr(III) Solid Phases by Chlorine in Drinking Water

Michelle Chebeir[†] and Haizhou Liu^{*†}

[†] Department of Chemical and Environmental Engineering, University of California at
Riverside, Riverside, CA 92521 USA

* Corresponding author, e-mail: haizhou@engr.ucr.edu, phone (951) 827-2076, fax
(951) 827-5696.

Submitted to Environmental Science & Technology

Table of Contents

Text S1: Synthesis of chromium hydroxide $\text{Cr}(\text{OH})_{3(s)}$	4
Text S2: Standard redox potential calculation for $\text{Cr}(\text{III})$ solids.....	5
Text S3: Calculation on bromide catalytic effects	7
Text S4: Kinetics Model Prediction on $\text{Cr}(\text{VI})$ formation in drinking water	8
Table S1 Summary of redox potential of different redox couples at pH 7.	9
Figure S1 Experiments on the adsorption and desorption of $\text{Cr}(\text{VI})$ on $\text{Cr}(\text{OH})_{3(s)}$. Initial $[\text{Cr}(\text{OH})_{3(s)}]=2.8\text{ mM}$, initial $[\text{Cr}(\text{VI})]=0.22\text{ mM}$. Ionic strength= 10 mM	10
Figure S2 Measurements of free chlorine by DPD method. The interference caused by the presence of $\text{Cr}(\text{VI})$ was eliminated when the DPD method was modified with the addition of thioacetamide.	11
Figure S3 Measurements of $\text{Cr}(\text{VI})$ by DPC method. The possible interference caused by the presence of chlorine was eliminated when the DPD method was modified with the addition of ammonium sulfate.....	12
Figure S4 Effect of initial $\text{Cr}(\text{III})$ -to-chlorine molar ratio on the $\text{Cr}(\text{III})$ oxidation by chlorine. (A) Chlorine consumption; (B) $\text{Cr}(\text{VI})$ formation with time on $\text{Cr}(\text{OH})_{3(s)}$ oxidation. $\text{Cr}(\text{III})\text{:Cl}_2$ ratio was varied. Initial $[\text{Cr}(\text{III})]=0.28\text{ mM}$. Ionic strength= 10 mM . pH= 7	13
Figure S6 Impact of pH on the oxidation of $\text{Cr}_2\text{O}_3(s)$ by chlorine. (A) Chlorine consumption profile; (B) $\text{Cr}(\text{VI})$ formation profile. Initial $[\text{Cl}_2]=20\text{ mg/L}$ as Cl_2 , $[\text{Cr}_2\text{O}_3(s)]=2.8\text{ mM}$, molar ratio of $\text{Cr}(\text{III})\text{:Cl}_2=10\text{:}1$, ionic strength= 10 mM	15
Figure S7 Impact of pH on the oxidation of $\text{Cr}(\text{OH})_{3(s)}$ by chlorine. (A) Chlorine consumption profile; (B) $\text{Cr}(\text{VI})$ formation profile. Initial $[\text{Cl}_2]=20\text{ mg/L}$ as Cl_2 , $[\text{Cr}(\text{OH})_{3(s)}]=2.8\text{ mM}$, molar ratio of $\text{Cr}(\text{III})\text{:Cl}_2=10\text{:}1$, ionic strength= 10 mM	16
Figure S8 Change in zeta potential with pH for all three $\text{Cr}(\text{III})$ solids. pH was varied by adding varying amounts of HClO_4 and NaOH . Ionic strength= 10 mM . Suspension of $\text{Cr}(\text{III})$ solids= 0.2 g/L	17
Figure S9 Cumulative $\text{Cr}(\text{VI})$ formation vs. Cl_2 consumption at varying pHs for $\text{Cr}_2\text{O}_3(s)$ oxidation by chlorine. Molar ratio of $\text{Cr}(\text{III})\text{:Cl}_2$ was $10\text{:}1$ with the initial concentration of $\text{Cr}(\text{III})$ at 2.8 mM . Ionic strength of solution was 10 mM NaClO_4 . pH was regulated with 0.05 mM HClO_4 and NaOH . The theoretical stoichiometric molar ratio of $\Delta\text{Cr}(\text{VI})\text{:}\Delta\text{Cl}_2$ is 0.67	18
Figure S10 Cumulative $\text{Cr}(\text{VI})$ formation vs. Cl_2 consumption at varying pHs for $\text{Cu}_2\text{Cr}_2\text{O}_5(s)$. Molar ratio of $\text{Cr}(\text{III})\text{:Cl}_2$ was $10\text{:}1$ with the initial concentration of $\text{Cr}(\text{III})$ at	

2.8 mM. Ionic strength of solution was 10 mM NaClO ₄ . pH was regulated with 0.05 mM HClO ₄ and NaOH..	19
Figure S13 Impact of bromide concentration on the oxidation of Cr(OH) _{3(s)} by chlorine. (A) Chlorine consumption profile; (B) Cr(VI) formation profile. [Cl ₂]=20 mg/L as Cl ₂ , [Cr(OH) _{3(s)}]=2.8 mM, Cr(III):Cl ₂ =10:1, pH=7.5	22
Figure S14 Impact of bromide concentration on the oxidation of Cu ₂ Cr ₂ O _{5(s)} by chlorine. (A) Chlorine consumption profile; (B) Cr(VI) formation profile. [Cl ₂]=20 mg/L as Cl ₂ , [Cu ₂ Cr ₂ O _{5(s)}]=2.8 mM, Cr(III):Cl ₂ =10:1, pH=7.5	23
Figure S16 Correlation between cumulative Cr(VI) formation and cumulative chlorine consumption Δ[Cl ₂] in the presence of bromide during the oxidation of Cr(OH) _{3(s)} by chlorine. Initial [Cr(OH) _{3(s)}]=2.8 mM, molar ratio of Cr(III):Cl ₂ =10:1, [Br ⁻]=5 mg/L, ionic strength=10 mM,. pH=7.0.	25
Figure S17 Stoichiometry of Cr(VI) formation with HOBr consumption during the oxidation of Cr(III) _(s) by HOBr. (A) Cu ₂ Cr ₂ O _{5(s)} ; (B) Cr ₂ O _{3(s)} . Initial [HOBr]=280 μM, molar ratio of Cr(III)/Cl ₂ =10:1, pH=7.0, ionic strength=10 mM.	26
Figure S18 Kinetics model prediction of enhanced Cr(VI) formation via Cr(III) solid phases oxidation by chlorine due to the catalytic effect of bromide in U.S. source waters. (A) Cr(VI) formation via Cr(OH) _{3(s)} oxidation; (A) Cr(VI) formation via Cr ₂ O _{3(s)} oxidation.	27
References	28

Text S1: Synthesis of chromium hydroxide $\text{Cr}(\text{OH})_{3(s)}$

Chromium nitrate nonahydrate $\text{Cr}(\text{NO}_3)_3 \cdot 9\text{H}_2\text{O}$ (Acros Organics) was brought to a pH of 10 using 1 M sodium hydroxide NaOH at which $\text{Cr}(\text{OH})_{3(s)}$ precipitated. The suspension was then magnetically stirred for 24 hours to fully precipitate out Cr(III) hydroxide. Following that, the suspension was transferred to 50 mL tubes and centrifuged (Beckman Coulter Avant JE) at 3000 G for 5 minutes. The supernatant was decanted and a new batch of DI water was added for centrifugation. This cleaning procedure was repeated for 8 times until the supernatant reached a pH 7, indicating all impurities had been removed. The purified $\text{Cr}(\text{OH})_3$ particles were then dried with a freeze dryer (VirTis Benchtop SLC). Acid digestion and ICP-MS were conducted in order to determine the presence of hydrates. The resulting formula of the synthesized Cr(III) solid was $\text{Cr}(\text{OH})_3 \cdot 2\text{H}_2\text{O}$. XRD was performed in order to determine the crystallinity of each of the solids.

Text S2: Standard redox potential calculation for Cr(III) solids

The standard redox potential (E^o) for each of the three Cr(III) solids was calculated as:

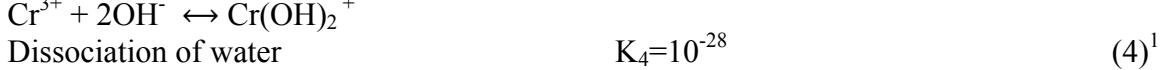
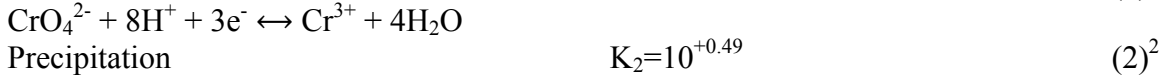
$$E^o = (0.059)pe^o$$

pe^o represents the equilibrium constant of a redox reaction in which the oxidant gains one electron. K is the equilibrium constant of a redox reaction in which the oxidant gains n_e of electrons.

$$pe^o = \frac{1}{n_e} \log K$$

pe^o represents the standard redox potential in which the reduced species releases one electron and K is the equilibrium rate constant.

The standard redox potential of amorphous $\text{Cr}(\text{OH})_{3(s)}$ is calculated as follows:



Combine Reactions 1 to 4:



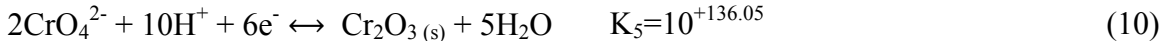
$$pe^o = \frac{1}{3} (\log K) = \frac{1}{3} (67.84) = 22.61$$

$$E^o = 1.33 \text{ V}$$

The standard redox potential of chromium oxide $\text{Cr}_2\text{O}_{3(s)}$ is calculated as follows:



Combine Reactions 6 to 9:

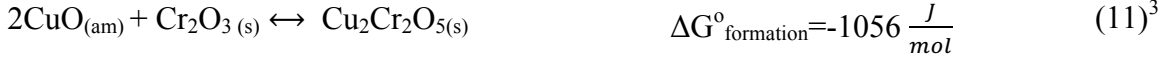


$$pe^o = \frac{1}{6} (\log K) = \frac{1}{6} (136.05) = 22.67$$

$$E^o = 1.34 \text{ V}$$

The standard redox potential of copper chromite $\text{Cu}_2\text{Cr}_2\text{O}_{5(s)}$ is calculated as follows:

First, the equilibrium constant K must be calculated:



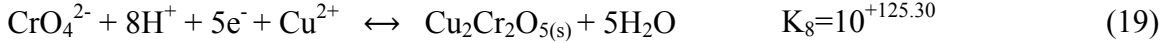
$$\Delta G^\circ = -RT \ln K = (-8.314 \frac{\text{J}}{\text{mol} \cdot \text{K}})(298\text{K}) (\ln K)$$

$$\ln K = 0.4262$$

Oxidation potential calculation using calculated K:



Combine Reactions 12 to 18



$$pe^0 = \frac{1}{6} (\log K) = \frac{1}{6} (136.05) = 22.67$$

$$E^0 = 1.337 \text{ V}$$

To calculate the redox potential (E) for $\text{CrO}_4^{2-}/\text{Cr}(\text{OH})_3(s)$ in typical drinking water conditions (Table S1), Nernst equation was applied:

$$pe = \frac{1}{n_e} \log \frac{\{Red\}}{\{Ox\}} + \frac{n_H}{n_e} pH - pe^0$$

$$pe = \frac{1}{3} \log \frac{\{Cr(III)\}}{[\{Cr(VI)\} = 1 \times 10^{-10} \text{ mM}]} + \frac{5}{3} (7) - 22.16 = 7.70$$

$$E = \frac{7.70}{0.059} = 0.13 \text{ V}$$

The rest of the redox potentials were calculated and listed in Table S2.

For example, in typical drinking water conditions – 2 mg/L of chlorine, 7 mg/L of chloride and pH at 7 – the redox potential of HOCl/Cl^- redox couple is 1.41 V. This is much higher than the redox potentials of $\text{CrO}_4^{2-}/\text{Cr(III)}_{(s)}$ for all three Cr(III) solids, with 0.16 V, 0.16 V and 0.20 V for $\text{Cr}(\text{OH})_3(s)$, $\text{Cr}_2\text{O}_3(s)$ and $\text{Cu}_2\text{Cr}_2\text{O}_{5(s)}$, respectively (Text S2).

Text S3: Calculation on bromide catalytic effects

The first-order rate constant of HOBr decay (0.0553 min^{-1} calculated from the slope of data in Figure S11) was divided by the concentration of Cr(III) in the system (2.8 mM) to get a second order rate of $19.8 \text{ M}^{-1} \text{ s}^{-1}$ (referred to as $k_{\text{formation}}$).

Mass balance on bromide:

$$\frac{d[\text{Br}^-]}{dt} = k_{\text{formation}}[\text{HOBr}][\text{Cr(III)}_{(s)}] - k_{\text{consumption}}[\text{HOCl}][\text{Br}^-]$$

At steady-state condition, $\frac{d[\text{Br}^-]}{dt} = 0$. Therefore:

$$\frac{[\text{HOBr}]_{ss}}{[\text{Br}^-]_{ss}} = \frac{k_{\text{consumption}}[\text{HOCl}]_t}{k_{\text{formation}}[\text{Cr(III)}_{(s)}]_t}$$

At initial experimental conditions, $[\text{HOCl}]_i = 0.28 \text{ mM}$ and $[\text{Cr(III)}]_i = 2.8 \text{ mM}$. From literature and experimental calculations, $k_{\text{consumption}} = 1550 \text{ M}^{-1} \text{ s}^{-1}$ and $k_{\text{formation}} = 19.8 \text{ M}^{-1} \text{ s}^{-1}$, respectively. Therefore:

$$\frac{[\text{HOBr}]_{ss}}{[\text{Br}^-]_{ss}} = \frac{(1550)(1)}{(19.75)(10)} = 7.85$$

A value of 7.85 indicates that the steady state concentration of HOBr is significantly greater than the steady state concentration of Br^- in the system.

Text S4: Kinetics Model Prediction on Cr(VI) formation in drinking water

Considering a drinking water distribution system with a residual chlorine of 0.3 mg/L and a Cr(III) solid of 100 µg/L, this level of chlorine residual is within the typical concentration range of disinfectant residual in distribution system, and the level of Cr(III) still meets the EPA regulation on total Cr level (Maximum Contamination Level = 100 µg/L). Based on the second-order reaction kinetics model established in this study, Cr(VI) formation in drinking water from Cr(III) solid oxidation by chlorine can be predicted as a function of residence time in the distribution system:

$$Cr(VI) = Cr(III)_{(s),initial} \{1 - \exp(-k_{Cr(VI)} (S_{Cr(III)(s)}) [MW_{Cr(III)(s)}] [HOCl]_{TOT} t)\}$$

$Cr(III)_{(s),initial}$ is the initial concentration of a particular type of residual Cr(III) solid in drinking water distribution system (100 µg/L). $k_{Cr(VI)}$ is the surface area normalized rate constant of Cr(VI) formation ($L \cdot m^{-2} \cdot s^{-1}$). $S_{Cr(III)(s)}$ is the BET surface area of a particular Cr(III) solid (m^2/g). $MW_{Cr(III)(s)}$ is the molecular weight of the corresponding Cr(III) solid (g/mol). $[HOCl]_{TOT}$ is the total concentration of free chlorine including both hypochlorous acid (HOCl) and hypochlorite ion (OCI^-), *i.e.*, $[HOCl]_{TOT} = [HOCl] + [OCI^-]$ (mol/L). t is the residence time of distributions system.

Table S1 Summary of redox potential of different redox couples at pH 7.

Chemical Species	Redox Potential (V) in Typical Drinking Water Chemical Condition *	Redox Potential (V) in Initial Experimental Condition **	Redox Potential (V) in Final Experimental Condition ***
HOCl/Cl ⁻	1.41	1.42	1.40
CrO ₄ ²⁻ /Cr(OH) _{3(s)}	0.16	0.13	0.16
CrO ₄ ²⁻ /Cr ₂ O _{3(s)}	0.16	0.13	0.17
CrO ₄ ²⁻ /Cu ₂ Cr ₂ O _{5(s)}	0.20	0.17	0.21

* Typical drinking water chemical conditions: [Cl₂]=2 mg/L, [Cl⁻]=7 mg/L and [Cr(VI)] =10 µg/L.

** Initial experimental condition: [Cl₂]=20 mg/L, and [Cl⁻]=20 mg/L and [Cr(VI)] = 1×10⁻⁵ µg/L.

*** Final Experimental Condition: [Cl₂]=0.2 mg/L,[Cl⁻]=20 mg/L and [Cr(VI)] =10 mg/L.

The activity of Cr(III) solid phases was chosen as 1.0 in all conditions because it predominantly exists as a solid in aqueous solutions at the pHs studied in this work. The activity of solid phases is assumed to be 1.0⁴. Detailed calculations on the standard redox potentials are shown in Text S2.

Throughout the course of the reaction, the oxidation potential of the HOCl/Cl⁻ redox couple is always greater than that of each of the three Cr(III) solids. This relationship holds in typical drinking water chemical conditions. Therefore, the experimental conditions did not change the thermodynamics boundary of the redox system compared to drinking water conditions.

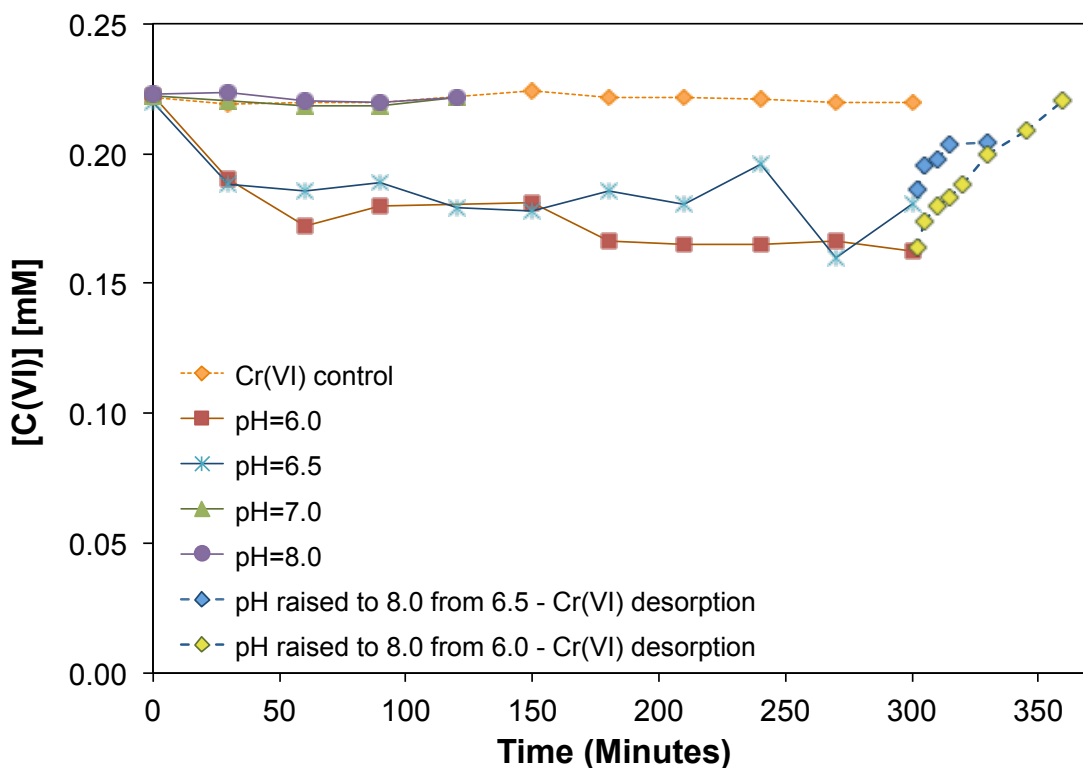


Figure S1 Experiments on the adsorption and desorption of Cr(VI) on $\text{Cr}(\text{OH})_{3(s)}$. Initial $[\text{Cr}(\text{OH})_{3(s)}] = 2.8 \text{ mM}$, initial $[\text{Cr}(\text{VI})] = 0.22 \text{ mM}$. Ionic strength = 10 mM.

The adsorption of Cr(VI) on $\text{Cr}(\text{OH})_{3(s)}$ was negligible when the solution pH was equal or above 7.0, as shown by the Cr(VI) measurements at pHs 7.0 and 8.0. Approximately 20% of Cr(VI) was absorbed on $\text{Cr}(\text{OH})_{3(s)}$ when the solution pH was below 7.0, as shown in the Cr(VI) measurements at pHs 6.5 and 6.0. The adsorbed Cr(VI) was recovered by increasing the solution pH to 8.0. For example, when the solution pH was raised from 6.5 to 8.0, 100% of the Cr(VI) was recovered in 45 minutes.

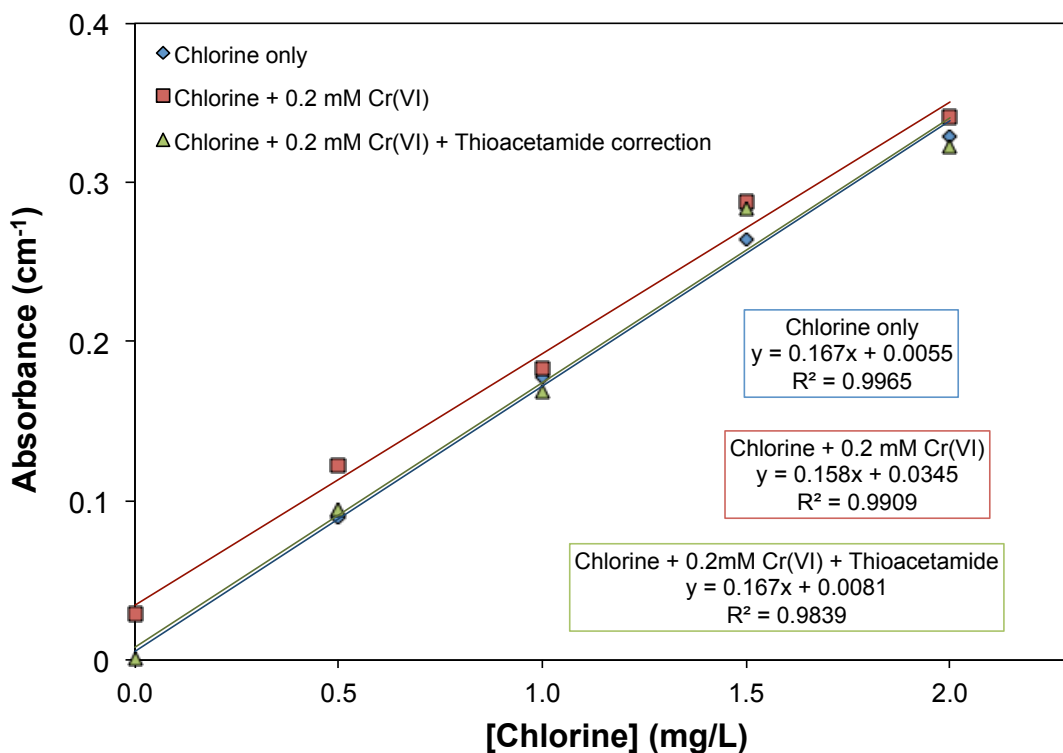


Figure S2 Measurements of free chlorine by DPD method. The interference caused by the presence of Cr(VI) was eliminated when the DPD method was modified with the addition of thioacetamide.

The standard DPD colorimetric method for chlorine measurement can be subject to interference caused by Cr(VI). This interference comes from the oxidation of DPD by Cr(VI). To account for any Cr(VI) interference in DPD, thioacetamide was added to quench chlorine and quantify any absorbance induced by Cr(VI). For example, when 0.2 mM Cr(VI) coexisted with chlorine, the difference of absorbance in the samples without thioacetamide addition (red square dots in Figure S2) and the ones with thioacetamide addition (green triangle dots) was contributed by Cr(VI). This is seen by the upward shift in the y-axis values (red squares vs. green triangles). When thioacetamide was added (green triangles), this interference was effectively removed as the y-axis values were the same as the ones in samples without Cr(VI) (green triangles vs. blue diamonds). In all samples taken from actually oxidation experiments, the amount of Cr(VI) was much lower than 0.2 mM Cr(VI). Therefore, chlorine concentration was accurately measured without Cr(VI) interference in all experimental samples.

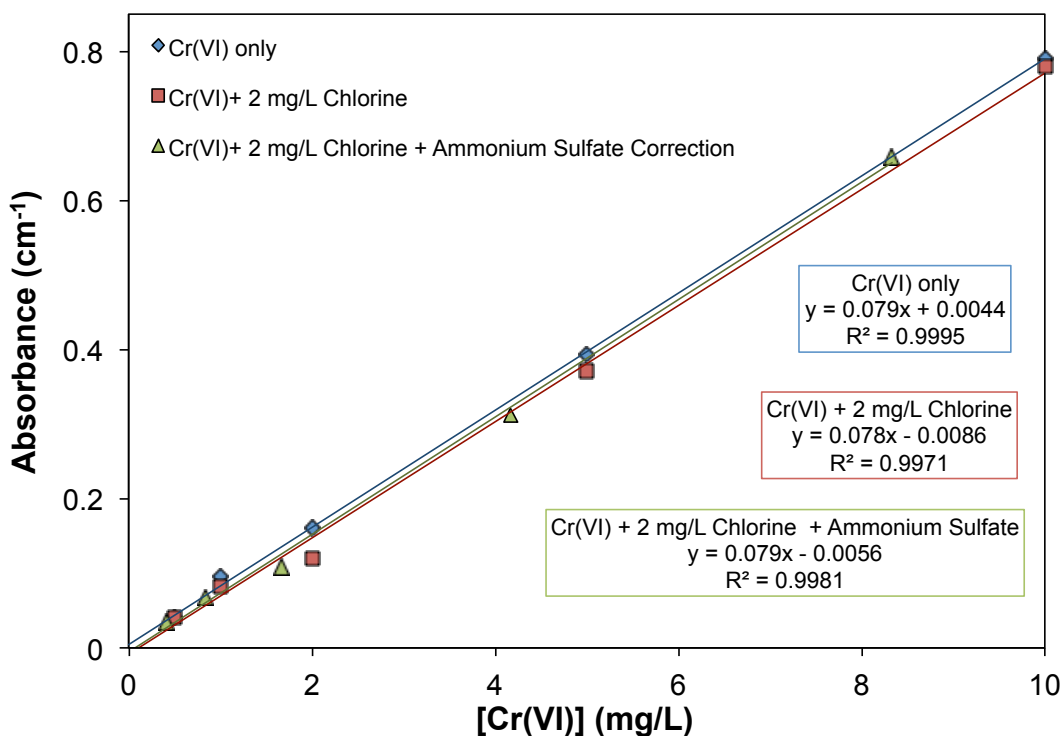


Figure S3 Measurements of Cr(VI) by DPC method. The possible interference caused by the presence of chlorine was eliminated when the DPD method was modified with the addition of ammonium sulfate.

The standard DPC colorimetric method for Cr(VI) measurement could be subject to interference caused by chlorine. This interference may come from the oxidation of DPC by chlorine. Results showed that chlorine did not cause a significant interference on Cr(VI) measurement, as indicated by the difference of absorbance between the samples with chlorine (red square dots in Figure S3) and the one without chlorine (blue diamond dots). The addition of ammonium sulfate quenched any possible interference from chlorine, allowing for an accurate reading of the Cr(VI) absorbance, as indicated by the green triangle dots. The addition of ammonium sulfate converted chlorine to chloramine. Chloramine did not oxidize DPC within the time scale of measurements and possible chlorine interference was eliminated.

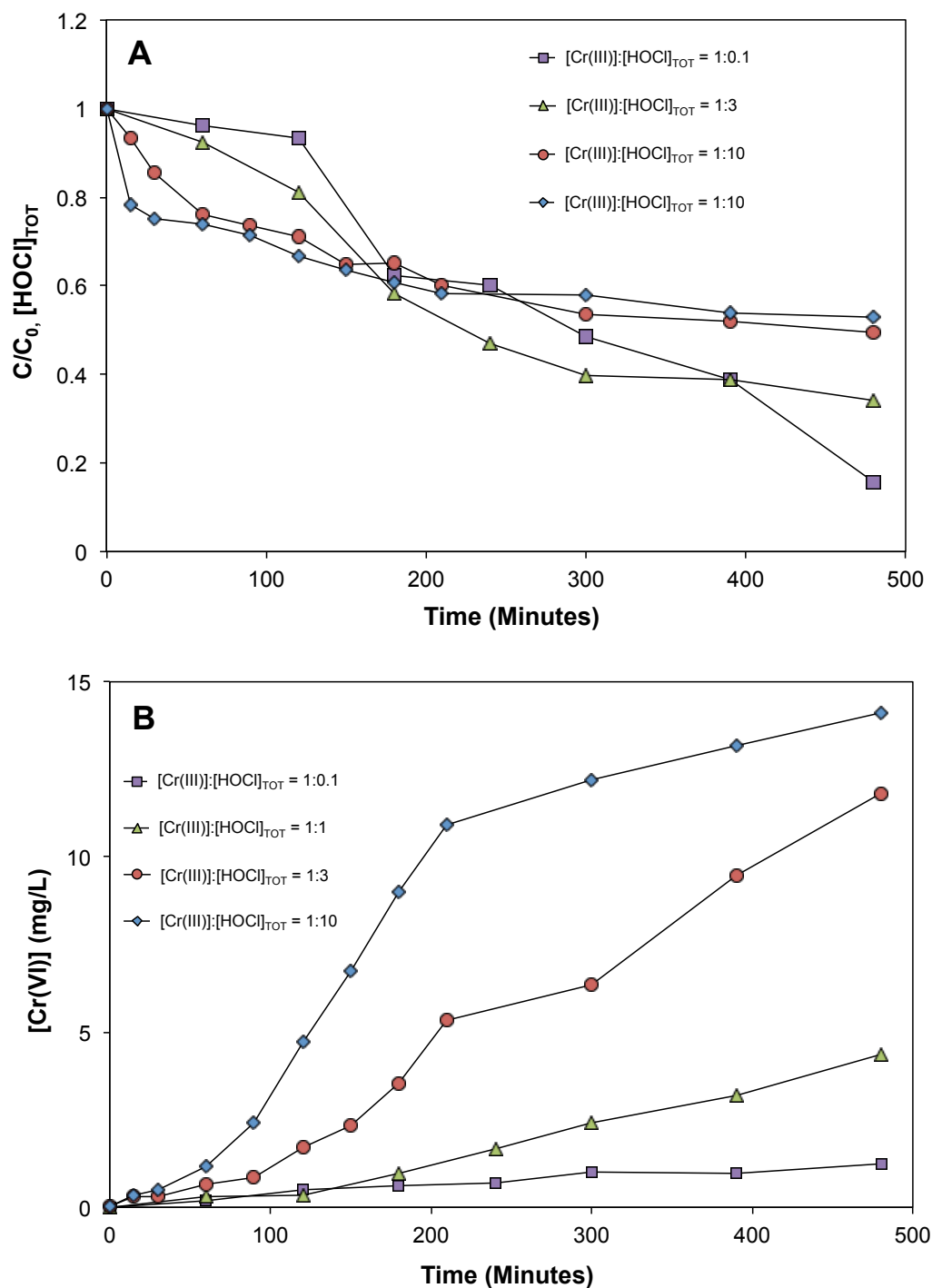


Figure S4 Effect of initial Cr(III)-to-chlorine molar ratio on the Cr(III) oxidation by chlorine. (A) Chlorine consumption; (B) Cr(VI) formation with time on $Cr(OH)_3(s)$ oxidation. Cr(III): Cl_2 ratio was varied. Initial $[Cr(III)] = 0.28$ mM. Ionic strength = 10 mM. pH = 7.

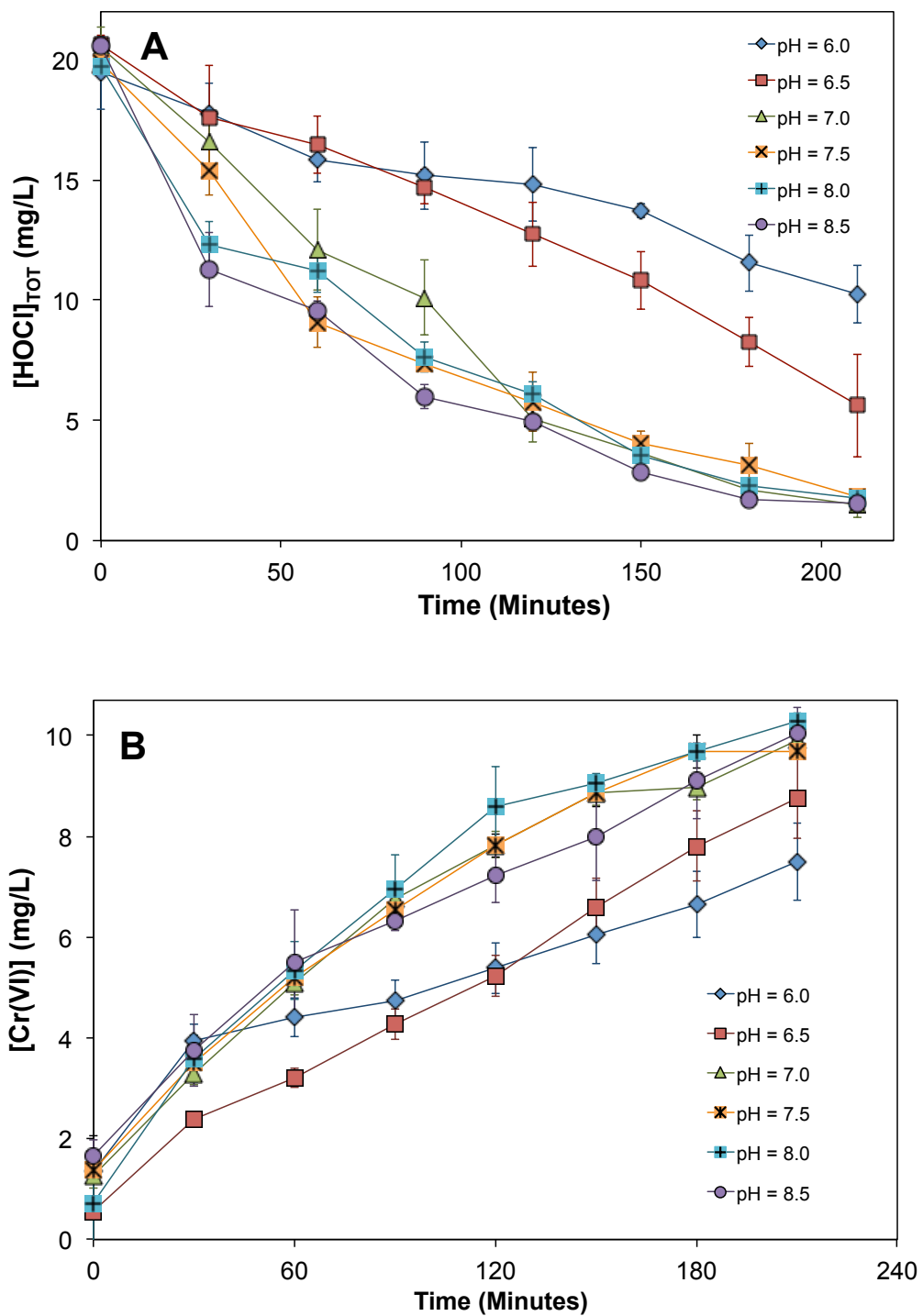


Figure S5 Impact of pH on the oxidation of $\text{Cu}_2\text{Cr}_2\text{O}_{5(\text{s})}$ by chlorine. (A) Chlorine consumption profile; (B) Cr(VI) formation profile. Initial $[\text{HOCl}]_{\text{TOT}} = 20$ mg/L as Cl_2 , $[\text{Cu}_2\text{Cr}_2\text{O}_{5(\text{s})}] = 2.8$ mM, molar ratio of Cr(III)/ $\text{Cl}_2 = 10:1$, ionic strength = 10 mM.

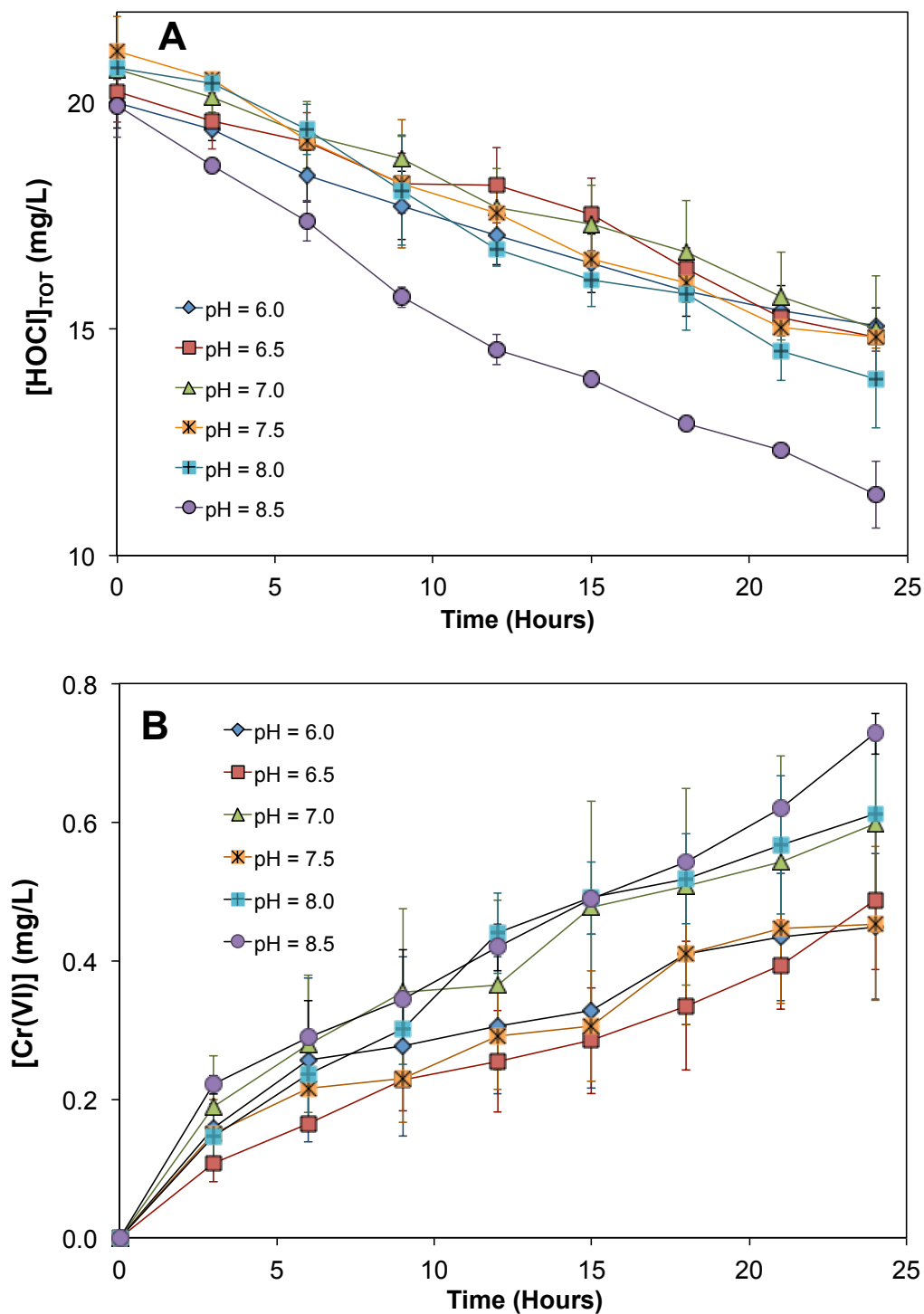


Figure S6 Impact of pH on the oxidation of $\text{Cr}_2\text{O}_3(\text{s})$ by chlorine. (A) Chlorine consumption profile; (B) Cr(VI) formation profile. Initial $[\text{HOCl}]_{\text{TOT}}=20$ mg/L as Cl_2 , $[\text{Cr}_2\text{O}_3(\text{s})]=2.8$ mM, molar ratio of $\text{Cr(III)}:\text{Cl}_2=10:1$, ionic strength=10 mM.

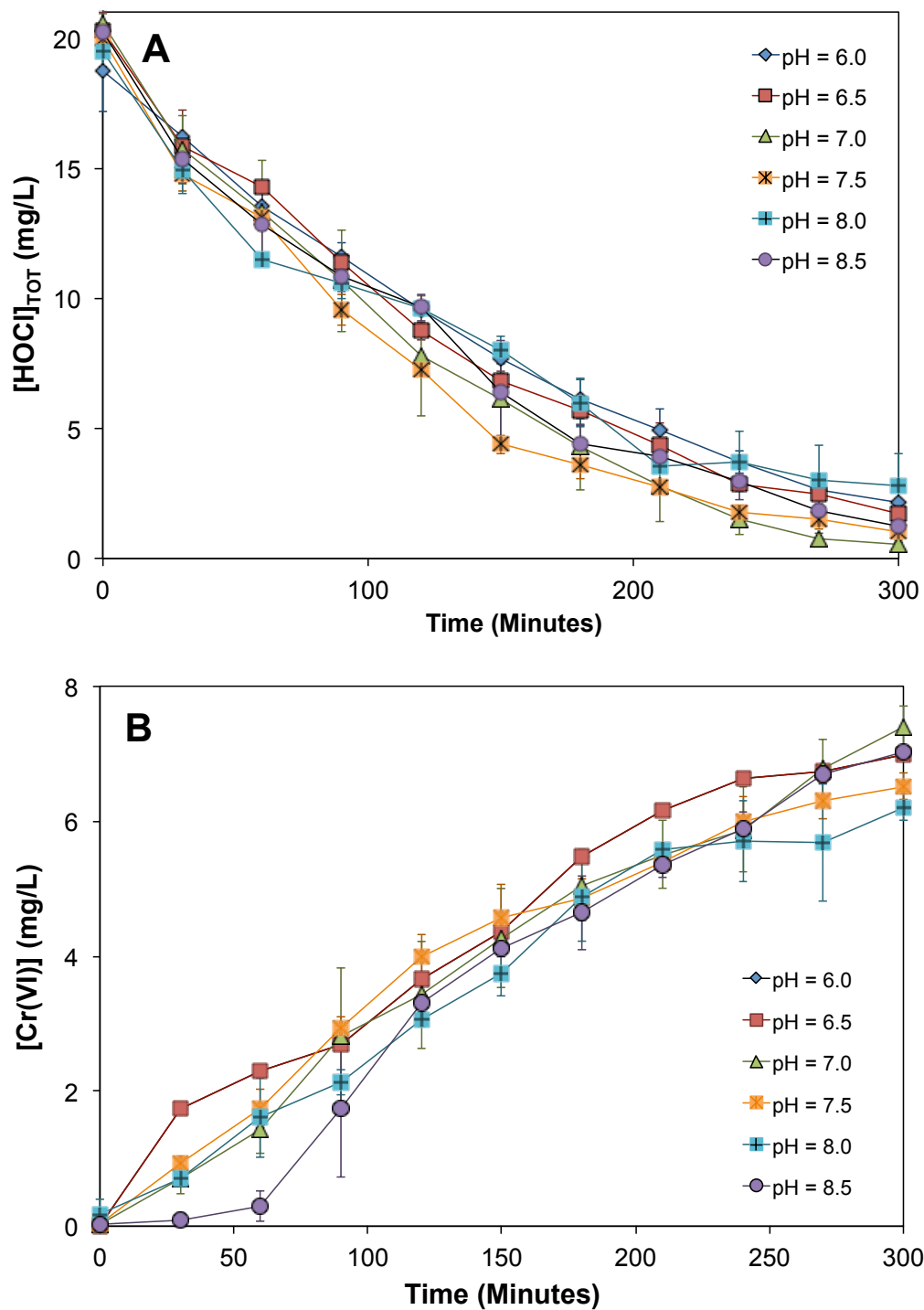


Figure S7 Impact of pH on the oxidation of $\text{Cr(OH)}_{3(s)}$ by chlorine. (A) Chlorine consumption profile; (B) Cr(VI) formation profile. Initial $[\text{HOCl}]_{\text{TOT}} = 20$ mg/L as Cl_2 , $[\text{Cr(OH)}_{3(s)}] = 2.8$ mM, molar ratio of $\text{Cr(III)}:\text{Cl}_2 = 10:1$, ionic strength = 10 mM.

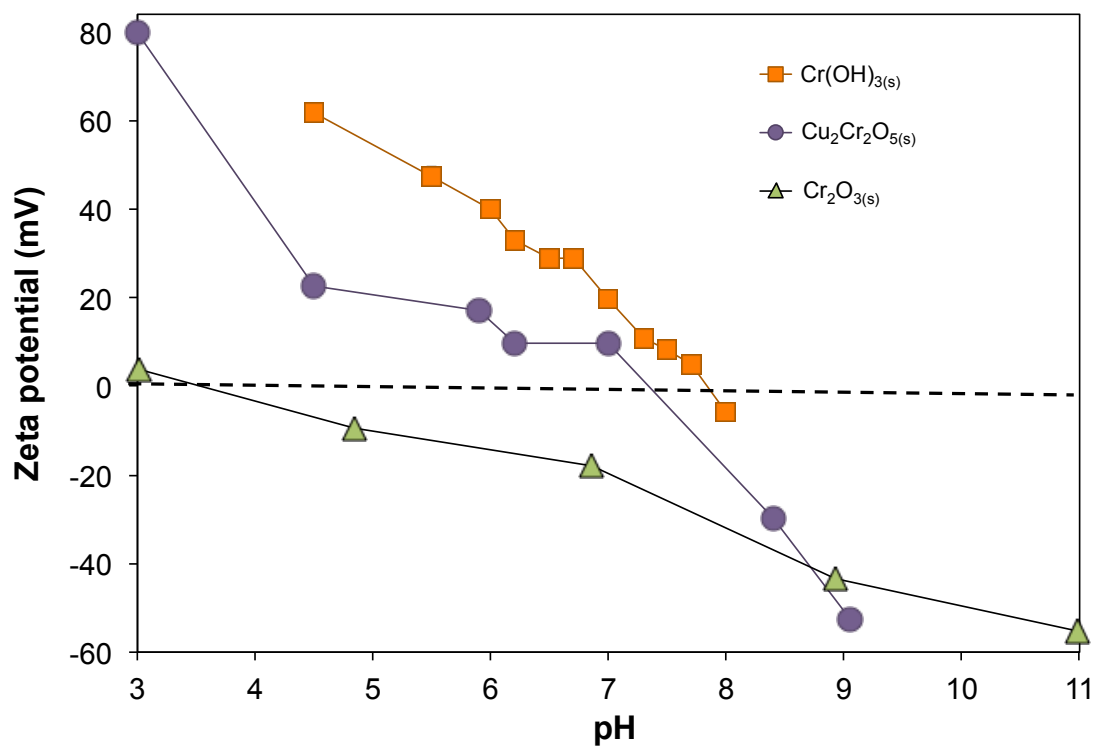


Figure S8 Change in zeta potential with pH for all three Cr(III) solids. pH was varied by adding varying amounts of HClO_4 and NaOH . Ionic strength=10 mM. Suspension of Cr(III) solids=0.2 g/L.

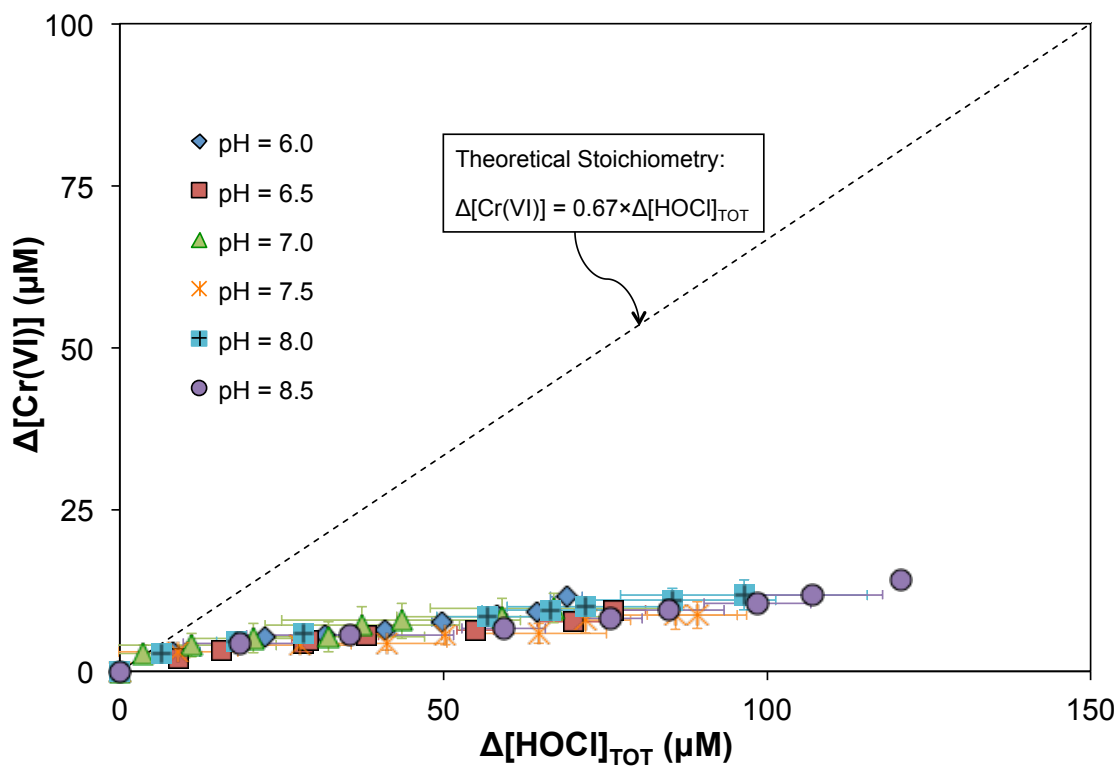


Figure S9 Cumulative Cr(VI) formation vs. Cl_2 consumption at varying pHs for $\text{Cr}_2\text{O}_{3(\text{s})}$ oxidation by chlorine. Molar ratio of Cr(III): Cl_2 was 10:1 with the initial concentration of Cr(III) at 2.8 mM. Ionic strength of solution was 10 mM NaClO_4 . pH was regulated with 0.05 mM HClO_4 and NaOH. The theoretical stoichiometric molar ratio of $\Delta[\text{Cr(VI)}]:\Delta[\text{HOCl}]_{\text{TOT}}$ is 0.67.

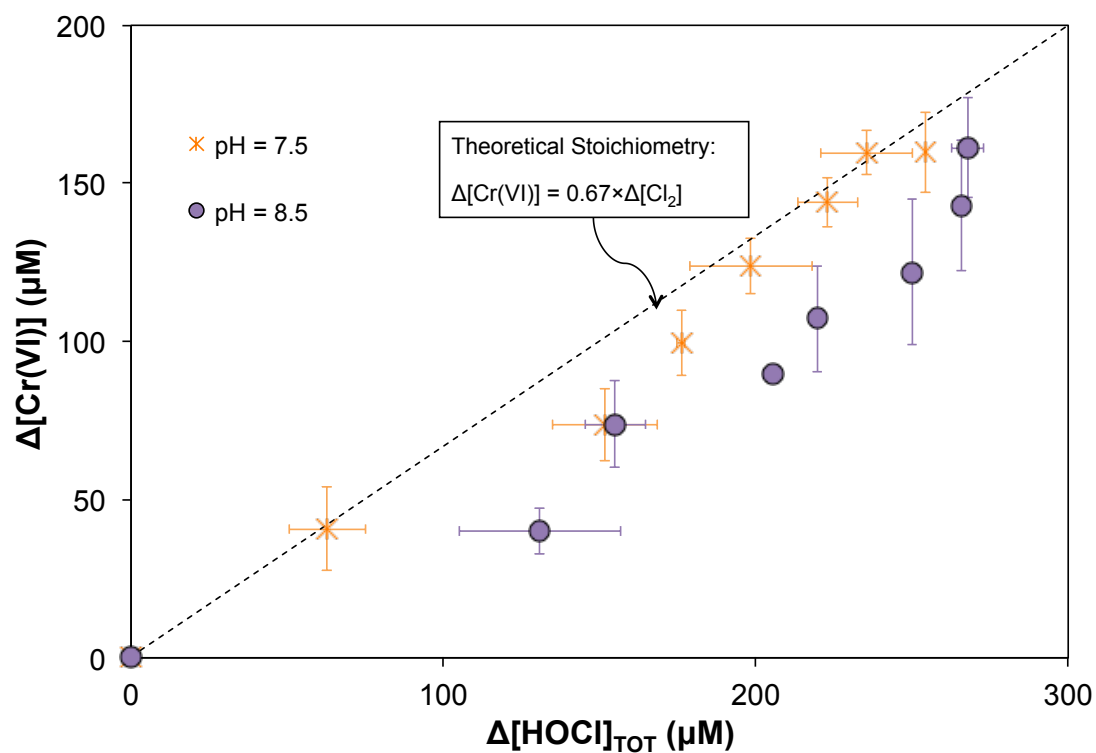


Figure S10 Cumulative Cr(VI) formation vs. Cl_2 consumption at varying pHs for $\text{Cu}_2\text{Cr}_2\text{O}_5(\text{s})$. Molar ratio of Cr(III): Cl_2 was 10:1 with the initial concentration of Cr(III) at 2.8 mM. Ionic strength of solution was 10 mM NaClO_4 . pH was regulated with 0.05 mM HClO_4 and NaOH. The theoretical stoichiometric molar ratio of $\Delta[\text{Cr(VI)}]:\Delta[\text{HOCl}]_{\text{TOT}}$ is 0.67.

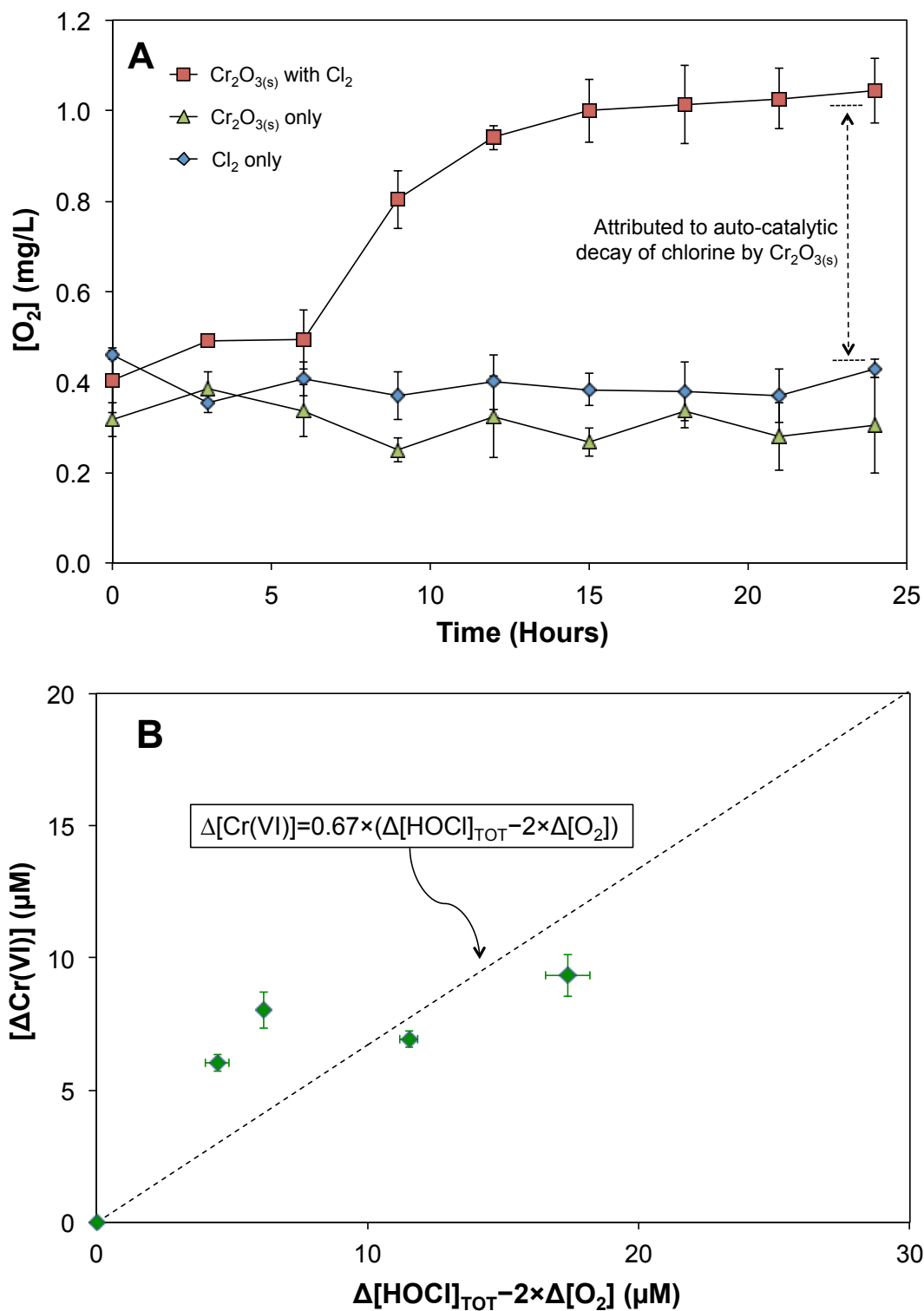


Figure S11 Oxidation of $\text{Cr}_2\text{O}_{3(s)}$ by chlorine. (A) Dissolved O_2 profile; (B) Revised stoichiometry of Cr(VI) formation considering catalytic decay of chlorine. Initial $[\text{HOCl}]_{\text{TOT}} = 20 \text{ mg Cl}_2/\text{L}$, molar ratio of Cr(III)/ $\text{Cl}_2 = 10:1$, pH=7.0, ionic strength=10 mM.

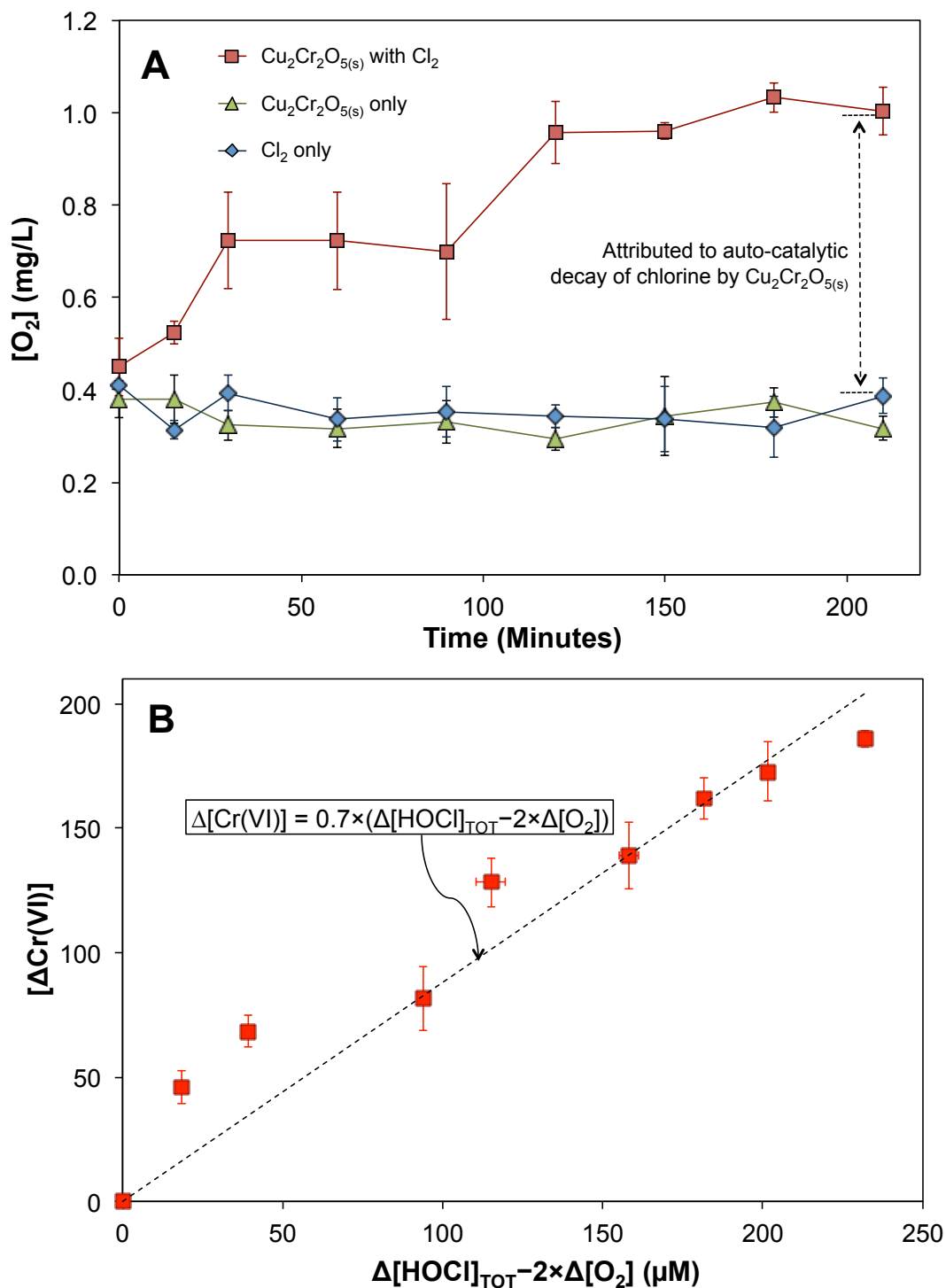


Figure S12 Oxidation of $\text{Cu}_2\text{Cr}_2\text{O}_{5(s)}$ by chlorine. (A) Dissolved O_2 profile; (B) Revised stoichiometry of Cr(VI) formation considering catalytic decay of chlorine. Initial $[\text{HOCl}]_{\text{TOT}} = 20 \text{ mg Cl}_2/\text{L}$, molar ratio of $\text{Cr(III)}/\text{Cl}_2 = 10:1$, $\text{pH} = 7.0$, ionic strength = 10 mM.

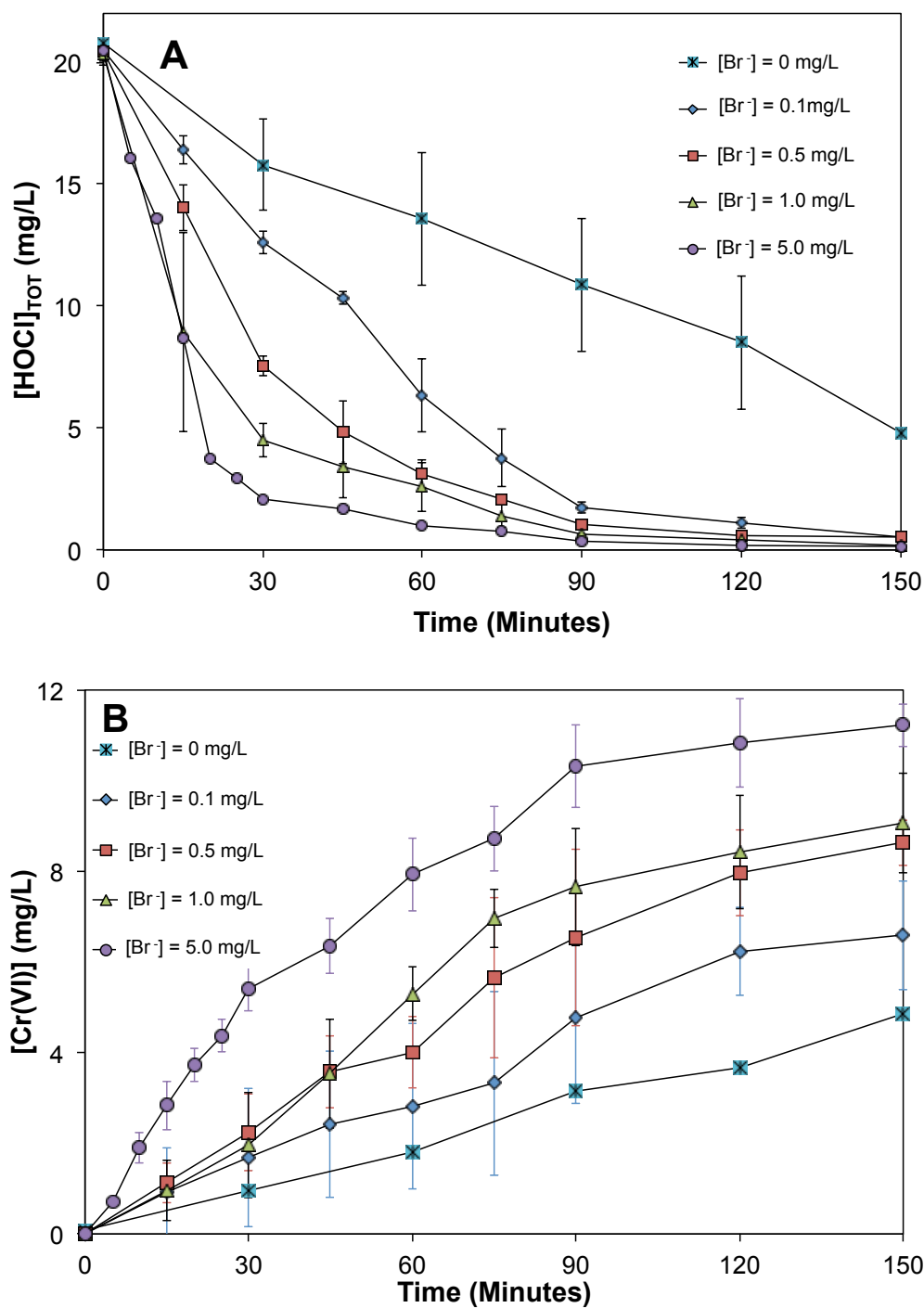


Figure S13 Impact of bromide concentration on the oxidation of $\text{Cr(OH)}_3(\text{s})$ by chlorine. (A) Chlorine consumption profile; (B) Cr(VI) formation profile. $[\text{HOCl}]_{\text{TOT}} = 20 \text{ mg/L}$ as Cl_2 , $[\text{Cr(OH)}_3(\text{s})] = 2.8 \text{ mM}$, $\text{Cr(III)}:\text{Cl}_2 = 10:1$, $\text{pH} = 7.5$

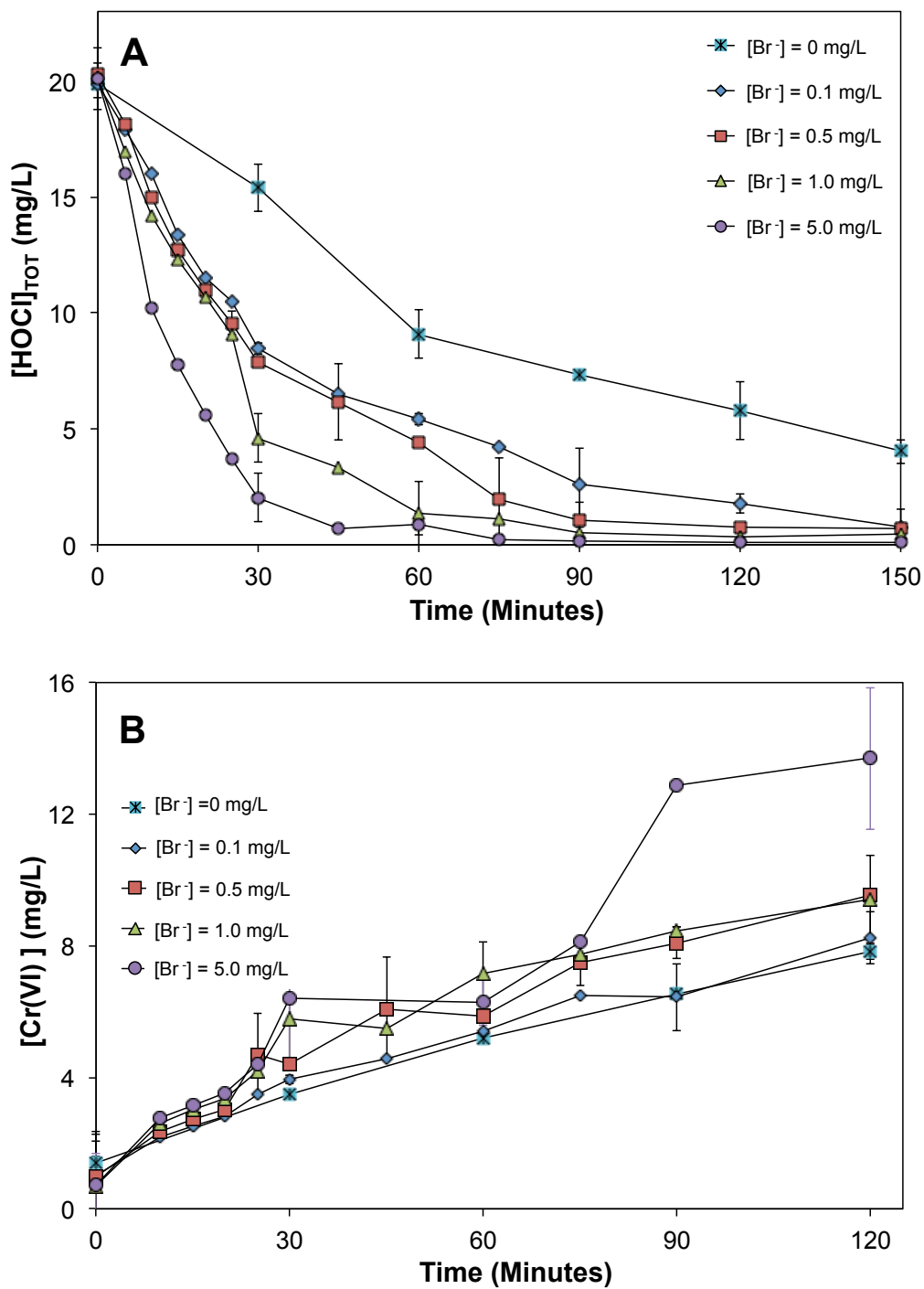


Figure S14 Impact of bromide concentration on the oxidation of $\text{Cu}_2\text{Cr}_2\text{O}_{5(\text{s})}$ by chlorine. (A) Chlorine consumption profile; (B) Cr(VI) formation profile. $[\text{HOCl}]_{\text{TOT}} = 20 \text{ mg/L}$ as Cl_2 , $[\text{Cu}_2\text{Cr}_2\text{O}_{5(\text{s})}] = 2.8 \text{ mM}$, $\text{Cr(III)}:\text{Cl}_2 = 10:1$, $\text{pH} = 7.5$

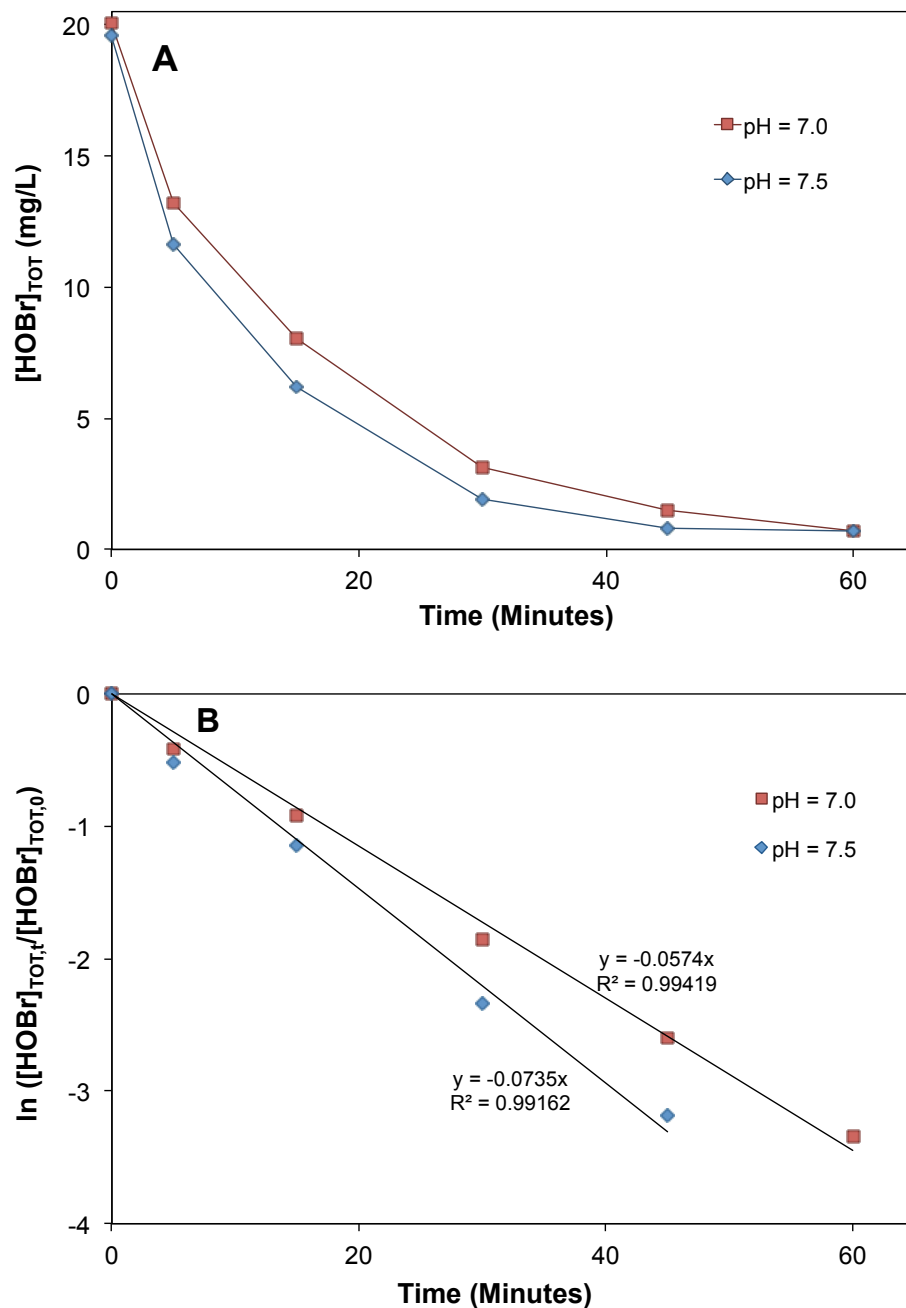


Figure S15 The reaction kinetics of oxidation of $\text{Cr}(\text{OH})_{3(s)}$ by HOBr at pH 7 and 7.5. (A) Consumption of HOBr with time; (B) Correlation of HOBr consumption rate with a first-order reaction kinetics. Initial $[\text{HOBr}]_{\text{TOT}} = 0.28 \text{ mM}$, molar ratio of $\text{Cr}(\text{III})$:HOBr = 10:1. Ionic strength = 10 mM. The pseudo first-order rate constants from Figure S14B was divided by the molar concentration and BET surface area of $\text{Cr}(\text{OH})_{3(s)}$ to obtain the second-order rate constants of 1.2 and $1.5 \times 10^{-3} \text{ L} \cdot \text{m}^{-2} \cdot \text{min}^{-1}$ at pH 7.0 and 7.5, respectively. This value is referred to as $k_{\text{formation}}$ in Text S3.

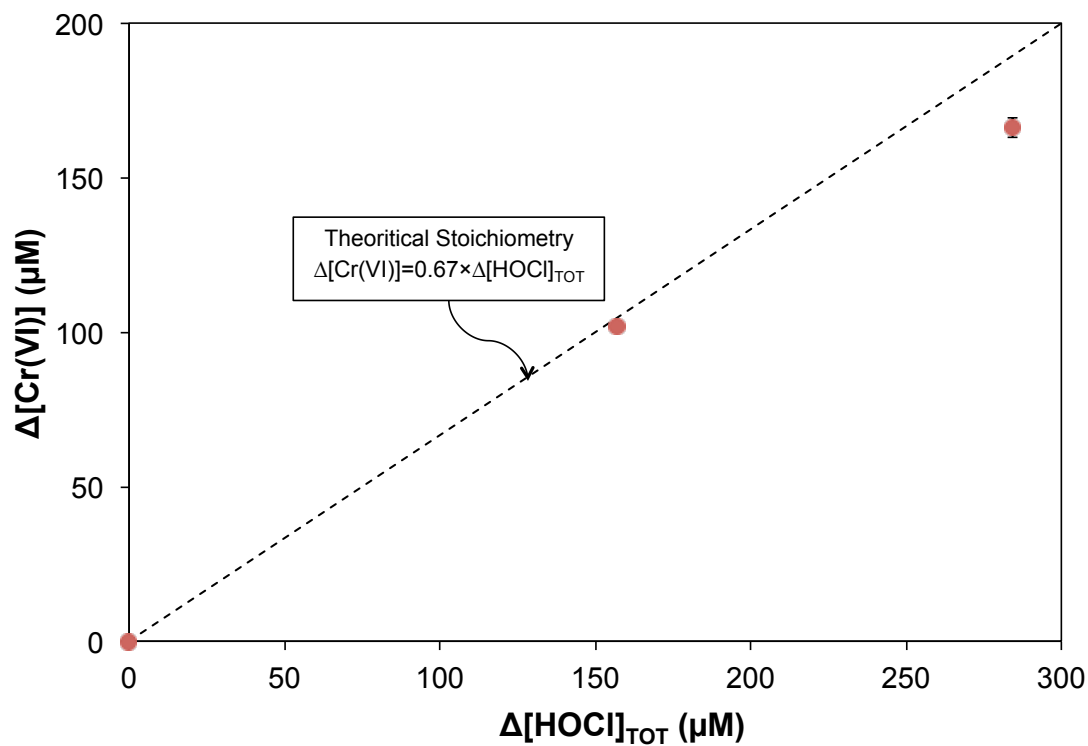


Figure S16 Correlation between cumulative Cr(VI) formation and cumulative chlorine consumption $\Delta[\text{Cl}_2]$ in the presence of bromide during the oxidation of $\text{Cr}(\text{OH})_{3(\text{s})}$ by chlorine. Initial $[\text{Cr}(\text{OH})_{3(\text{s})}] = 2.8 \text{ mM}$, molar ratio of $\text{Cr(III)}:\text{Cl}_2 = 10:1$, $[\text{Br}^-] = 5 \text{ mg/L}$, ionic strength = 10 mM, pH = 7.0.

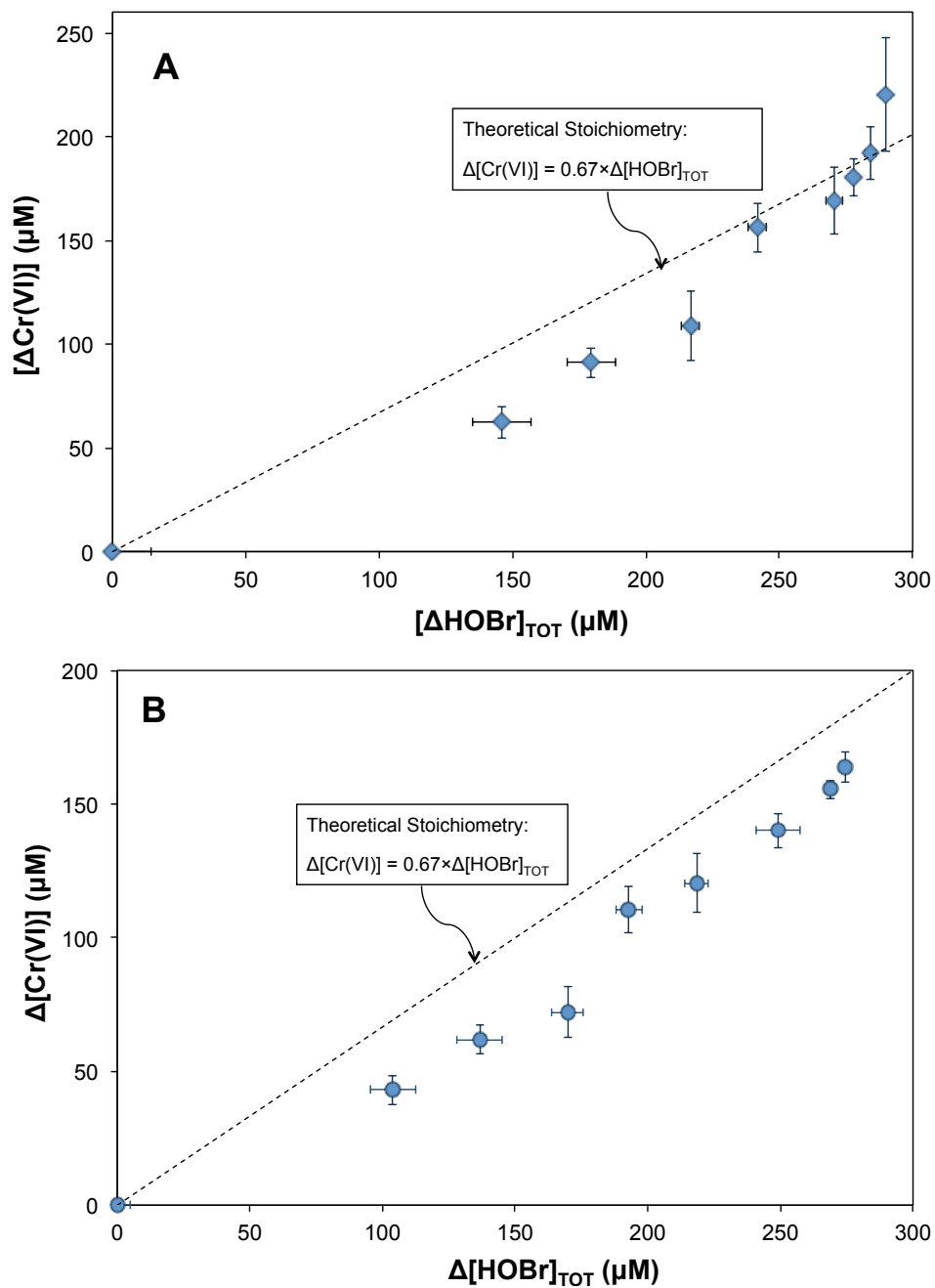


Figure S17 Stoichiometry of Cr(VI) formation with HOBr consumption during the oxidation of Cr(III)_(s) by HOBr. (A) Cu₂Cr₂O_{5(s)}; (B) Cr(OH)_{3(s)}. Initial [HOBr]_{TOT}=280 μM, molar ratio of Cr(III):Br₂=10:1, pH=7.0, ionic strength=10 mM.

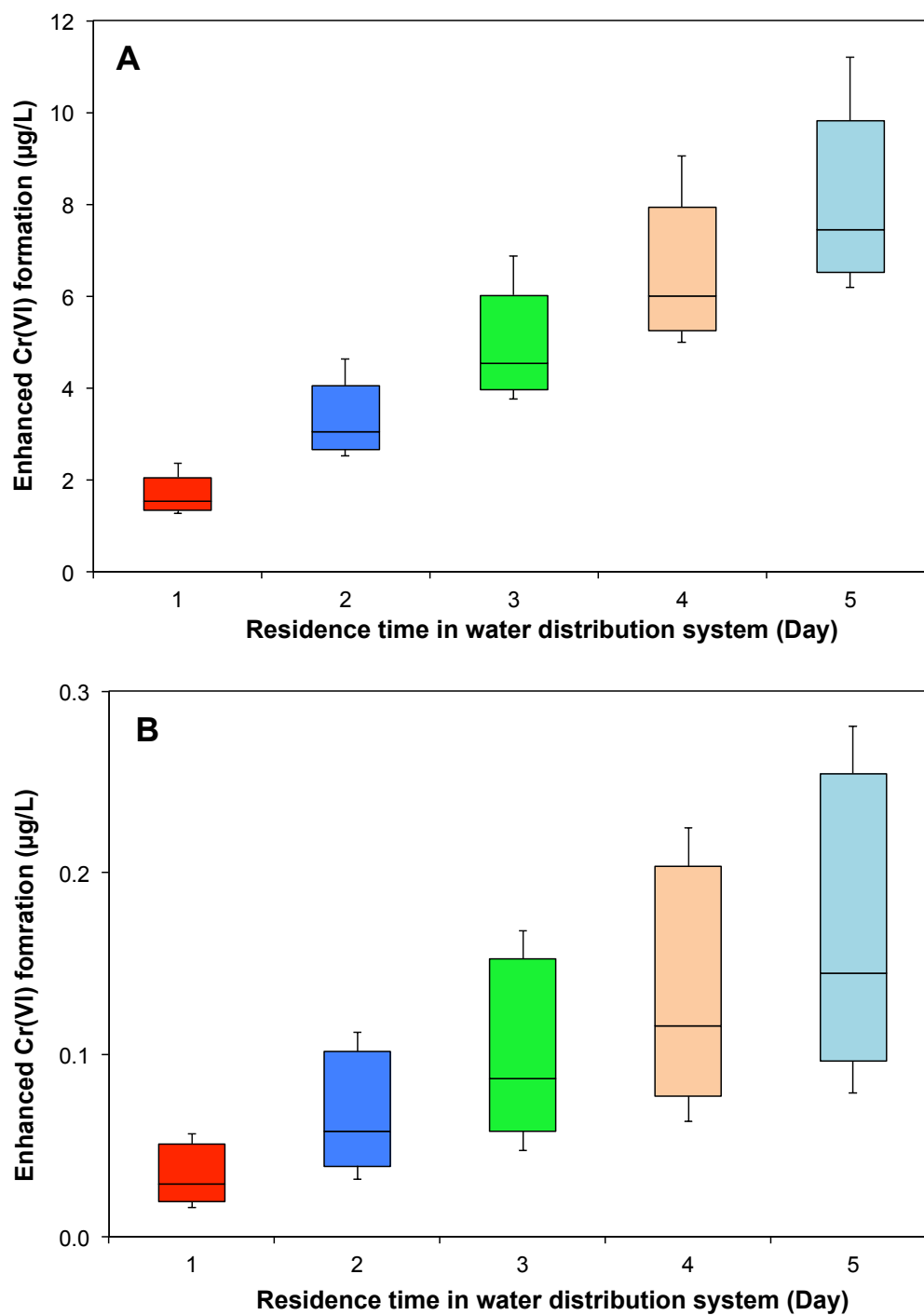


Figure S18 Kinetics model prediction of enhanced Cr(VI) formation via Cr(III) solid phases oxidation by chlorine due to the catalytic effect of bromide in U.S. source waters. (A) Cr(VI) formation via $\text{Cr}(\text{OH})_{3(s)}$ oxidation; (A) Cr(VI) formation via $\text{Cr}_2\text{O}_{3(s)}$ oxidation.

References

- 1 Benjamin, M.M. *Water Chemistry 2nd Edition*; Waveland Press Inc. Long Grove, IL, 2015.
- 2 Visual Minteq Software Database. <http://vminteq.lwr.kth.se> (accessed on 7/10/2015).
- 3 Jacobs, K.T. Gibbs energy of formation of CuCrO_4 and phase relations in the system Cu-Cr-O below 735 K. *Thermochimica Acta*. **1992**, 208, 341-348.